MOLECULAR ECOLOGY

Molecular Ecology (2016) **25**, 306–323 doi: 10.1111/mec.13385

DETECTING SELECTION IN NATURAL POPULATIONS: MAKING SENSE OF GENOME SCANS AND TOWARDS ALTERNATIVE SOLUTIONS

The population genomics of rapid adaptation: disentangling signatures of selection and demography in white sands lizards

STEFAN LAURENT,*†[1] SUSANNE P. PFEIFER,*†[1] MATTHEW L. SETTLES,‡ SAMUEL S. HUNTER,‡ KAYLA M. HARDWICK,‡ LOUISE ORMOND,*† VITOR C. SOUSA,†¶ JEFFREY D. JENSEN*† and ERICA BREE ROSENBLUM‡§

*School of Life Sciences, École Polytechnique Fédérale de Lausanne (EPFL), EPFL SV IBI-SV UPJENSEN, Station 15, CH-1015 Lausanne, Switzerland, †Swiss Institute of Bioinformatics (SIB), Lausanne, Switzerland, ‡Institute for Bioinformatics and Evolutionary Studies, University of Idaho, Moscow, ID 83844, USA, §Department of Environmental Sciences, Policy & Management, Berkeley, CA 94720, USA, ¶Institute of Ecology and Evolution, University of Berne, Baltzerstrasse 6, CH-3012 Berne, Switzerland

Abstract

Understanding the process of adaptation during rapid environmental change remains one of the central focal points of evolutionary biology. The recently formed White Sands system of southern New Mexico offers an outstanding example of rapid adaptation, with a variety of species having rapidly evolved blanched forms on the dunes that contrast with their close relatives in the surrounding dark soil habitat. In this study, we focus on two of the White Sands lizard species, *Sceloporus cowlesi* and *Aspidoscelis inornata*, for which previous research has linked mutations in the melanocortin-1 receptor gene (*Mc1r*) to blanched coloration. We sampled populations both on and off the dunes and used a custom sequence capture assay based on probed fosmid libraries to obtain >50 kb of sequence around *Mc1r* and hundreds of other random genomic locations. We then used model-based statistical inference methods to describe the demographic and adaptive history characterizing the colonization of White Sands. We identified a number of similarities between the two focal species, including strong evidence of selection in the blanched populations in the *Mc1r* region. We also found important differences between the species, suggesting different colonization times, different genetic architecture underlying the blanched phenotype and different ages of the beneficial alleles. Finally, the beneficial allele is dominant in *S. cowlesi* and recessive in *A. inornata*, allowing for a rare empirical test of theoretically expected patterns of selective sweeps under these differing models.

Keywords: adaptation, ecological genetics, molecular evolution, population genetics, reptiles

Received 9 May 2015; revision received 31 August 2015; accepted 4 September 2015

Introduction

The study of populations that have recently colonized novel environments has remained an area of particular interest in evolutionary biology – both because newly encountered environmental pressures can generate strong natural selection and because adaptation over short timescales can be detectable on the genomic level. However, recent and rapid colonization events are also frequently characterized by severe demographic perturbations (e.g. in population size and migration rates), which may obscure genomic patterns of selection (e.g. Przeworski 2002; Jensen *et al.* 2005; Thornton & Jensen 2007). Although various test statistics have been developed to circumvent this challenge (e.g., Nielsen *et al.* 2005; Jensen *et al.* 2007; Pavlidis *et al.* 2012), the

Correspondence: Erica Bree Rosenblum, Fax: +1 510 643 5438; E-mail: rosenblum@berkeley.edu

[1]These authors contributed equally to the work.

performance of these approaches is often poor under the demographic scenarios associated with colonization, particularly for cases of severe population bottlenecks and ongoing gene flow (Crisci *et al.* 2013; Poh *et al.* 2014). As a result, the underlying demographic history of a population should be explicitly modelled when searching for targets of natural selection.

Although disentangling selection and demography remains difficult, the use of population-level, genome-scale data from recently diverged natural populations can help to discern the relative impact of these factors. The advent of next-generation sequencing technologies together with new computational and statistical techniques to model demographic histories (Thornton & Andolfatto 2006; Gutenkunst *et al.* 2009; Excoffier & Foll 2011; Naduvilezhath *et al.* 2011; Mathew & Jensen 2015) have enabled more accurate inference of demographic history, which can then be used as a null model when scanning for genomic targets of selection. As a result, substantial advances have been made in detecting genes contributing to phenotypic changes in populations that have undergone recent adaptation in the wild such as *Drosophila*, stickleback, mice and humans (e.g., Reusch *et al.* 2001; Ihle *et al.* 2006; Domingues *et al.* 2012; Linnen *et al.* 2013) and during domestication (e.g., Doebley 2004; Pollinger *et al.* 2005; reviewed in Stinchcombe & Hoekstra 2008; Ellegren & Sheldon 2008; Mackay *et al.* 2009; Stapley *et al.* 2010). However, even in these cases, the underlying genetic variants responsible for the observed changes often remain difficult to identify (Chan *et al.* 2010).

Melanin-based pigmentation has long been studied as a model for understanding adaptive evolution (Cott 1940; Norris & Lowe 1964), and pigmentation phenotypes are some of the best examples of adaptation where the underlying genetic variants are well characterized. Coloration is involved in a range of different biological processes from crypsis to mimicry to thermoregulation to sexual signalling, and melanin-based coloration is conserved across many taxa (Thayer 1909; Cott 1940; Norris 1967; Kettlewell 1973; Majerus 1998; Bittner *et al.* 2002; Caro 2005). There are a number of genes that affect melanin-based phenotypes (Barsh 1996). Perhaps the most widely studied is the melanocortin-1 receptor gene (*Mc1r*), an important component of the melanin-synthesis signal transduction pathway in vertebrates (Barsh 1996). Mutations in the 1 kb coding region of *Mc1r* are responsible for colour variation in many species and have been investigated in domesticated animals [e.g. dogs (Newton *et al.* 2000), pigs (Kijas *et al.* 1998), horses (Marklund *et al.* 1996) and chickens (Takeuchi *et al.* 1996)] and in wild populations [e.g. mice (Nachman *et al.* 2003; Hoekstra *et al.* 2006), birds (Theron *et al.* 2001; Mundy *et al.* 2004), felines (Eizirik *et al.* 2003) and reptiles (Rosenblum *et al.* 2004)]. However, in many of the studied species, observed colour variation does not correspond to specific environmental pressures, making the connection of *Mc1r* variants to fitness unclear.

The White Sands system in southern New Mexico provides an opportunity to link colour variation in wild populations with adaptation to divergent habitats, and thus to understand the interplay between natural selection and population demography. White Sands is a distinctive landscape of stark white gypsum dunes (~275 square miles), which contrast dramatically with the dark substrate of the surrounding Chihuahuan Desert. There has been dramatic convergence in dorsal colour morphology by the White Sands fauna. All of the lizard species that inhabit White Sands and a subset of arthropods and mammals exhibit blanched forms on the gypsum dunes that contrast with dark forms in the rest of their ranges (Smith 1943; Lowe & Norris 1956; Rosenblum 2006). The light coloration of White Sands animals is likely an adaptation for crypsis to avoid detection by visually hunting avian predators, which preferentially predate on poorly background-matched prey (e.g. Dice 1947; Kaufman 1974; Luke 1989).

The demographic context in which natural selection has operated at White Sands has also been dynamic. The white habitat represents a geologically recent change in selective environment, with the bulk of the gypsum deposition having occurred within the last 7000 years (Langford 2003; Kocurek *et al.* 2007). Therefore, White Sands populations are expected to result from relatively recent colonizations. Moreover, there are no physical barriers separating White Sands from the surrounding dark desert soils, and the transition between white sand and dark soil habitats occurs abruptly. Thus, adaptation appears to have occurred in many species despite ongoing gene flow (Rosenblum & Harmon 2011).

Here, we use population-level genomic data to understand the demographic history and dynamics of natural selection at the genome level for dark and light populations of two White Sands lizards, the Southwestern Fence Lizard (*Sceloporus cowlesi*) and the Little Striped Whiptail (*Aspidoscelis inornata*). In each species, a single *Mc1r* amino acid substitution associated with blanched coloration has been identified through candidate gene studies and functional assays (Rosenblum *et al.* 2004, 2010). Population studies and functional assays have also demonstrated that the mutations have different dominance effects in the two species: the blanched allele appears to be dominant in *S. cowlesi* but recessive in *A. inornata* (Rosenblum *et al.* 2010). As a result, this system represents one of the first examples from a natural population where differing predictions regarding

hitchhiking effects of recessive and dominant mutations may be directly studied by comparing molecular signatures of natural selection for alleles of the same gene with different dominance effects in two species inhabiting the same novel environment.

In this study, we constructed fosmid libraries and developed a sequence capture approach to obtain >50 kb of sequence around *Mc1r* and hundreds of other random genomic locations in each species. We then use model-based statistical inference methods to infer the demographic history of the two populations using randomly selected genomic regions, investigate the evidence of selection around the candidate sites in *Mc1r*, estimate the age of these mutations relative to the geological age of White Sands and finally discuss these results in the light of existing population genetic theory. We find that White Sands and dark soil populations show only weak background genomic differentiation but display striking genetic differences in the *Mc1r* gene region. The patterns of variation that we observe at and around the *Mc1r* gene are consistent with strong selective sweeps caused by the nonsynonymous mutations previously associated with the blanched phenotype. Furthermore, the signatures of selection at *Mc1r* are consistent with the inferred dominance of the two beneficial mutations.

Material and methods

Population sampling

For both target species, we sampled populations from the two contrasting habitats (White Sands and dark soils) at the same localities for both *Aspidoscelis inornata* and *Sceloporus cowlesi* to enable demographic inference across the same spatial scale (Fig. 1). Populations are not polymorphic for colour; therefore, all individuals from White Sands exhibited the blanched phenotype, and all individuals from the dark soil sites exhibited the ancestral dark phenotype. We sampled White Sands individuals (referred to as 'WS' throughout) from White Sands National Monument (WSNM, Otero County, New Mexico), within an approximately 2 km radius along two neighbouring trails (Alkali Flat Trail and Backcountry Trail). We sampled dark soil individuals from two localities: (i) a Bureau of Land Management site northeast of white sands (BLM, Lincoln County, New Mexico; referred to as 'DS1' throughout), located ~85 km from WSNM with no separating geographic barrier in between, and (ii) from Jornada Long-term Ecological Research Station southwest of White Sands (JLTER, Doña Ana County, New Mexico; referred to as 'DS2' throughout), located ~50 km from White Sands but separated from WSNM by the San Andres

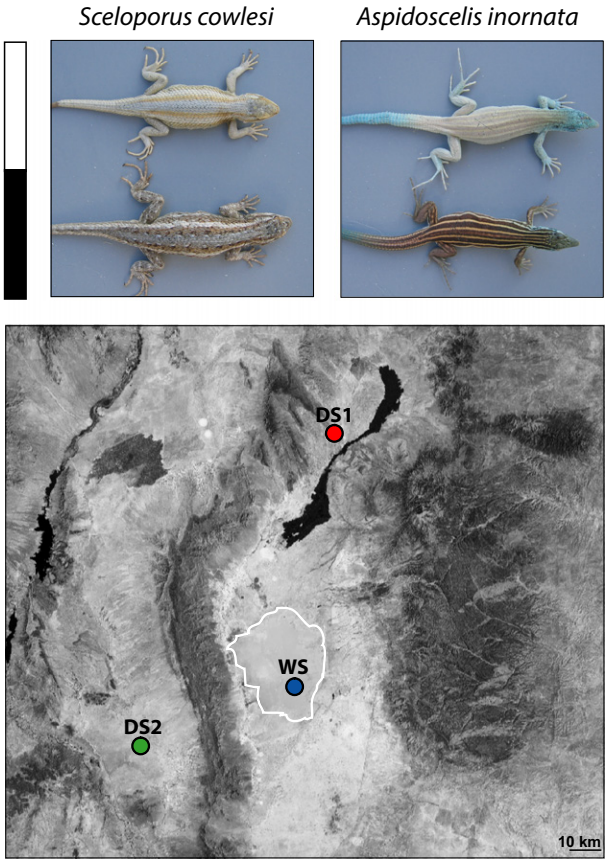

Fig. 1 Photographs and sampling localities for *Aspidoscelis inornata* and *Sceloporus cowlesi* from contrasting habitats. Blanched colour morphs are found at White Sands (indicated by the white bar) and dark colour morphs are found in the rest of the species' ranges (indicated by the black bar). Both species were sampled from the same three localities in New Mexico: White Sands National Monument (WS) in Otero County (blue), a dark soil Bureau of Land Management site (DS1) in Lincoln County (red) and a dark soil Jornada Long-term Ecological Research site (DS2) in Doña Ana County (green).

Mountains. The two focal species are patchily distributed in the Tularosa Basin, and the two dark soil sites represent the geographically closest localities where dark colour morphs of both species could reliably be sampled. We sampled approximately ten individuals per species per population.

Sequence capture assay

For each target lizard species, we first generated a fosmid library from high-quality DNA from a single White Sands individual. We used the diTag fosmid vector pFosDTx. The average *E. coli* insert size was approximately 40 kb, and each fosmid library contained ~5 million individual constructs. The fosmids were then colony-amplified, and we used homologous

recombination to screen the fosmid libraries for the *Mc1r* gene. We isolated clones that spanned a region up to 100 kb around the *Mc1r* gene and characterized these clones for insert size and target sequence presence. We also chose 96 random clones in each species. Fosmid library preparation and screening were done at the BACPAC Resources Center (Oakland, CA, USA).

We used both Roche 454 FLX+ pyrosequencing and Illumina MiSeq 2x150 bp sequencing to sequence the four *Mc1r* clones and the 96 random clones in each species. We processed raw sequences by removing any potential PCR duplicates, nontarget species sequence (e.g. from sequence adapters, PhiX spike-in, *E. coli* and fosmid vector) and by trimming low-quality ends. We merged Illumina paired-end reads with FLASH (Magoc & Salzberg 2011) and performed a hybrid (454 + Illumina) assembly using Roche GSASSEMBLER 2.6 (Roche 454, 2011). We retained contigs greater than 2 kb in length for further analysis resulting in 364 contigs for *A. inornata* (ranging from 2011 bp to 67 990 bp in length) and 290 contigs for *S. cowlesi* (ranging from 2309 bp to 54 334 bp in length). We combined the contigs into reference sequences, which we used to design capture probes for a custom Roche NimbleGen Capture Assay. The resulting probes covered more than 96% of our reference sequence contigs.

We extracted DNA from liver and tail samples using a DNeasy Blood and Tissue Kit (Qiagen). We generated Illumina TruSeq barcoded libraries for all individuals from each species, performed capture protocols according to the Roche NimbleGen specifications and sequenced using the Illumina MiSeq 2 × 150 bp and Illumina HiSeq 2 × 100 bp platforms.

Sequence alignment

Raw sequence reads (fastq files) were first preprocessed using a custom in-house pipeline including removal of PCR duplicates, contaminants (phiX) and Illumina sequencing adapters and trimming of low-quality bases (seqyclean parameter –qual 24 24) [GRC_Scripts, http://github.com/ibest/GRC_Scripts; Seqyclean, https://bitbucket.org/izhbannikov/seqyclean]. Preprocessed reads were aligned to the reference assembly for each lane separately using STAMPY (version 1.0.22) (Lunter & Goodson 2011). For every individual, aligned reads were merged across different lanes, proper pairs were extracted, and duplicate reads were removed using SAMTOOLS (Li *et al.* 2009), retaining only the read pair with the highest mapping quality. After mapping, the mean coverage across individuals was 112X in *A. inornata* (n = 32; Table S1a, Supporting information) and 115× in *S. cowlesi* (n = 28; Table S1b, Supporting information). The data set was limited to individuals with >20× coverage; this level of coverage has previously been shown to give good resolution for genotyping heterozygous sites within individual samples (The 1000 Genomes Project Consortium 2010). The resulting data set included 24 individuals for each species (i.e. *A. inornata*: 9 WS; 9 DS1; 6 DS2 and *S. cowlesi*: 9 WS; 9 DS1; 6 DS2). Because single nucleotide variants occur much more frequently than indels in the genomes of most species, most alignment algorithms annotate a single nucleotide variant rather than an indel at positions mismatching the reference genome when mapping individual reads. At positions of true indels, local misalignment of reads can produce an excess of false-positive SNP calls. To identify these positions and to improve variant calls, especially in low-complexity regions of the genome, a multiple sequence alignment was performed using the Genome Analysis Toolkit (GATK) IndelRealigner (McKenna *et al.* 2010; DePristo *et al.* 2011; Van der Auwera *et al.* 2013) to locally realign reads such that the number of mismatching bases is minimized across all reads spanning this locus.

Variant calling and filtering

Initial variant calls were made using GATK's HaplotypeCaller via local *de novo* assembly of haplotypes in an active region. Samples were genotyped jointly using GATK's GenotypeGVCFs tool. Besides true variation, these initial variant calls contain false positives due to systematic sequencing artefacts, mismapped reads and misaligned indels. Such false-positive calls often (i) exhibit excessive depth of read coverage, (ii) show an allelic imbalance, (iii) occur preferentially on a single strand, (iv) appear in regions of poor read alignment and (v) arise in unusual close proximity to multiple other variants. Thus, the majority of such calls can be detected and rejected using filters based on the above observations. Specifically, initial variant calls were filtered postgenotyping using GATK's VariantFiltration. Variants were removed using the following set of criteria (with acronyms as defined by the GATK package): (i) Three or more variants were found within 10 bp (clusterWindowSize = 10). (ii) The depth of coverage at the given position (summed across individuals) was <500 or >3000 (DP<500; DP>3000). (iii) There was evidence of a strand bias as estimated by Fisher's exact test (FS > 60.0) or the Symmetric Odds Ratio test (SOR > 1.0). (iv) The read mapping quality was low (MQ<80). (v) At least one of the samples was not called (NCC > 0).

After applying the initial filter criteria, the variant data set was limited to biallelic sites using VCFtools (Danecek *et al.* 2011). Genomic positions that fell within repeat regions of the reference assembly were excluded

because erroneous alignment of reads to these regions often leads to an increased frequency of heterozygous genotype calls. In particular, five different classes of repeats (i.e. LINE, LTR, DNA, simple repeats and low-complexity regions) were annotated using REPEATMASKER (Smit *et al.* 2013–2015) and variants within these regions were excluded from further analyses. To minimize genotyping errors, all variants with either missing data for any individual or genotype quality of less than 20 (corresponding to P[error] = 0.01) for any individual were excluded using VCFtools. Although hard genotype quality thresholds might cause an undercalling of heterozygotes in samples with low or moderate coverage, they have previously been shown to perform well in samples with >20× coverage (Nielsen *et al.* 2011). Variants were also filtered on the basis of Hardy–Weinberg Equilibrium (HWE). A *P*-value for HWE was calculated for each variant using VCFtools, and variants with $P < 0.01$ were removed. Sites for which all individuals were fixed for the nonreference allele were excluded using VCFtools. The resulting call sets contained 13 960 variants (407 SNPs within *Mc1r* and 13 553 within the random contigs) for *A. inornata* and 20 782 variants (691 SNPs within *Mc1r* and 20 091 within the random contigs) for *S. cowlesi*. Genotypes were phased using BEAGLE (version 4; Browning & Browning 2007).

Candidate variants were subject to several filter criteria to avoid false positives. As the applied filter metrics can lead to the exclusion of a substantial fraction of sites in the genome, mask files defining which nucleotides were accessible to variant discovery were generated to obtain the exact number of monomorphic sites in the reference assembly of each species (used in the demographic estimation) and to avoid biases when calculating summary statistics (e.g., π, Tajima's *D*, and weighted F_{st}). Mask files were created using the GATK pipeline described in the section 'Variant Calling and Filtering' with the exception that the '-allSites' flag was switched on when running GATK's GenotypeGVCFs tool to include all nonvariant loci for which there were data available. The same filter criteria were used with the exception of the variant cluster filter criteria, as this metric cannot be applied in cases of calls at every site in the genome. The filtering resulted in 58% and 45% of the reference assembly being accessible for *A. inornata* and *S. cowlesi*, respectively.

PCA, population structure and heterozygosity

For both species, variant data sets for the three populations were pruned for linkage, removing SNPs within a 50 SNP window that had $r^2 > 0.2$ (using '-indep 50 5 0.2' in plink) because both PCA (Zheng *et al.* 2012) and the inference of population structure require a set of independent SNPs. Population structure was studied using PCA and *structure* (Pritchard *et al.* 2000; Falush *et al.* 2003, 2007; Evanno *et al.* 2005; Hubisz *et al.* 2009), a software that identifies clusters of related individuals from multilocus genotyping data. *structure* analysis was performed with $K = 1$–5 (the number of clusters), using an admixture model with correlated allele frequencies. For each *K*, *structure* was run ten times for 10 000 steps after a burn-in period of 10 000 steps. The best *K* was chosen such that it maximized the marginal likelihood of the data. Previous work has shown that *structure* is able to identify isolated and relatively homogeneous groups even if they exhibit short divergence times or exchanges with other groups; this is because small, isolated populations often exhibit distinctive allele frequencies due to the fact that genetic drift occurs rapidly (Rosenberg *et al.* 2001). As a result, identified clusters often correspond well to geographically distinct population groups. Finally, heterozygosity was estimated based on the number of heterozygous SNPs per individual.

Demographic analyses

We explicitly evaluated different demographic scenarios for both *A. inornata* and *S. cowlesi*. Population modelling was done using two likelihood methods for comparison: (i) an approach that infers demographic parameters from the joint site frequency spectrum (SFS) using coalescent simulations (fastsimcoal2; Excoffier & Foll 2011; Excoffier *et al.* 2013) and (ii) a method in which the likelihood is calculated using a diffusion approximation (δaδi; Gutenkunst *et al.* 2009). SFS for all populations were directly generated from the final variant calls (vcf files) using an in-house script. As outgroup sequences were unavailable for *A. inornata* and *S. cowlesi*, we used the distribution of minor allele frequencies (i.e. the folded SFS) where the minor allele was considered to be the allele with the lowest frequency across all three populations. Monomorphic sites (defined as the set of all sites that passed all filtering criteria but for which no variants were called using GATK) were included in the analyses. For both species, we maximized the likelihood of the observed SFS under six complex demographic scenarios (three possible tree topologies each with two possible migration scenarios as described below; parameters shown in Table 2). We identified the best fitting demographic model on the basis of their Akaike's information criterion (AIC) score (Akaike 1974).

Given the genetic differentiation between populations identified by the PCA and *structure* analyses, for each species we tested the three possible tree topologies for the population set including WS, DS1 and DS2.

Topologies were tested both without migration and with asymmetrical migration between all population pairs. In the migration models, gene flow was only considered between *T*1 (the time of the most recent population split) and present. Additionally, admixture models were evaluated but in no case better fit the data. Effective population sizes were directly estimated by fixing the mutation rate to 1.5×10^{-9} (Olave *et al.* 2015). We also explored sensitivity of our results to assumptions about mutation rate (Table S2, Supporting information).

Fastsimcoal2 and δaδi were used on the folded SFS based on 13 553 SNPs and 20 091 SNPs outside *Mc1r* in *A. inornata* and *S. cowlesi*, respectively. For fastsimcoal2, the following options were used: -N 100000 (max. number of simulations), -L 40 (max. number of EM cycles), -M 0.001 (min. relative difference in parameter values for the stopping criterion). For every demographic model, 20 independent estimations with different initial parameter values were run, and results for the estimation with the highest likelihood are reported. For δaδi, 50 independent runs at different starting points were executed for each model. Generations were converted to years assuming a generation time of 1.5 years, a reasonable estimate for lizards in these taxonomic groups (e.g. Crenshaw 1955; Degenhardt *et al.* 1996). We also explored sensitivity of our results to assumptions about generation time (Table S2, Supporting information).

Selective sweep mapping in the Mc1r region

To test for a selective sweep around the *Mc1r* gene, we used the modification of the Kim & Stephan (2002) composite likelihood ratio (CLR) test proposed by Nielsen *et al.* (2005) as implemented in the software *SweeD* (Pavlidis *et al.* 2013). For each species, the folded SFS for all contigs except *Mc1r* was used as a neutral background reference and the CLR statistic was calculated at 10 000 grid points across the contig containing *Mc1r*. The CLR test assumes that the data were sampled at the end of the selective sweep; thus, following Meiklejohn *et al.* (2004), we excluded all WS individuals that were homozygous or heterozygous for the dark allele (as identified by Rosenblum *et al.* (2010)) from the analysis. The statistical thresholds for the test were defined as recommended by Nielsen *et al.* (2005). For each species, we simulated polymorphism data under our best demographic models (as estimated by *fastsimcoal2*) for the WS population and defined the threshold as the 95th percentile of the distribution of highest simulated CLR values.

Additionally, classical summaries of genetic diversity were calculated using a sliding window approach along the *Mc1r* region. We calculated π (nucleotide diversity), Tajima's *D* (Tajima 1989), and Weir and Cockerham's F_{st} (1984) using VCFtools (Danecek *et al.* 2011) taking into account the information about monomorphic sites (using the '–mask' option).

ABC estimation of selection coefficients and allele ages

To estimate selection coefficients and allele ages for the putatively selected mutations in *A. inornata* and *S. cowlesi*, we use the approximate Bayesian (ABC) approach of Ormond *et al.* (2015). In summary, an approximate Bayesian computation (ABC) approach was applied using a standard rejection algorithm and tolerance threshold of 0.01, implemented in the R program *abc* (Csillery *et al.* 2012), to estimate posterior distributions for selection strength *s* and allele age *T* in both WS populations. A total of 100 000 neutral and non-neutral simulations of the genealogies for White Sands populations in both species were generated using *msms* (Ewing & Hermisson 2010). Simulations used the demographically inferred N_e values, as well as the ρ and μ values used in demographic inference. The lengths *L* of the simulated sequences were taken to match the SNP data available around the region of the putatively selected mutation (a 65 kb region for *A. inornata* and a 54 kb region for *S. cowlesi*). The positions of the simulated selected mutations in both populations were chosen to match the position of the putative selection targets in the data sets. The prior distributions for the selection coefficient *s* and allele age *T* were $log_{10}(s) \sim U(-4, -0.5)$ and $log_{10}(T) \sim U(-4, -0.5)$, where U is a uniform distribution.

Simulated SNP patterns were output to the program *msstats* to calculate a panel of known summary statistics that are commonly used to characterize selective sweeps. Following Wegmann *et al.* (2009), a partial least squares (PLS) approach was applied to incorporate the most informative summary statistics from *msstats* into the ABC calculation and to filter out noise from uninformative statistics. Summary statistics were also calculated from the actual SNP data for White Sands populations in both species and transformed into PLS components using the same loadings as described above. Point estimates for *s* and *T* were calculated from the mode of the joint density posterior distribution using the two-dimensional kernel density function in the MASS package in R (Venables & Ripley 2002). Finally, credibility intervals were calculated using 95% of the marginal posterior distributions for *s* and *T*.

Results

Sequence capture

Our sequence capture approach resulted in a high-quality population-level data set. We recovered a large

contig containing *Mc1r* for both species. The *Mc1r* contig was 54 kb long and contained 691 SNPs in *Sceloporus cowlesi* and was 68 kb long and contained 407 SNPs in *Aspidoscelis inornata*. We also recovered 289 additional genomic contigs with an average length of 11.3 kb in *S. cowlesi* and 363 additional genomic contigs with an average length of 8.6 kb in *A. inornata*. These genomic contigs contained 20 091 SNPs in *S. cowlesi* and 13 553 SNPs in *A. inornata*.

Demographic analysis of the Aspidoscelis inornata populations

All three *A. inornata* populations exhibited similar levels of nucleotide diversity (0.15–0.18%, Table 1) and Tajima's *D* values (0.11–0.80) (calculated based on the genetic variation observed outside *Mc1r*). Weighted F_{st} values ranging from 0.11 (WS-DS2) to 0.15 (DS1-DS2) outside of *Mc1r* indicated genetic structure between populations. Genetic structure was also identified by the *structure* analysis – supporting the existence of three clusters, which exactly corresponded to the three sampled localities (Figs 2 and S1a, Supporting information). The PCA also showed clear separation of all three populations (Fig. 3). Notably, weighted F_{st} values were greatly elevated within *Mc1r* in comparisons between White Sands and dark soil populations [0.28 (WS-DS1), 0.36 (WS-DS2)], but not between the two dark soil populations [0.12 (DS1-DS2)].

The demographic model inferred as best fitting the data was the same in both fastsimcoal2 and δaδi (Fig. 4), with concordant parameter estimates between the two methods (Table 2). This model suggests a young divergence between WS and DS1 and an older split with DS2, as well as an absence of gene flow between populations. Predictive simulations were generated to test whether the demographic parameters inferred with the two methods were able to correctly predict the patterns of genetic variation observed in the *A. inornata* data set. The results of this analysis demonstrated that both models were well calibrated, predicting π, Tajima's *D* and F_{st} correctly in all three populations (Fig. S2, Supporting information) and the SFS of each individual population (Fig. S3, Supporting information).

Table 1 Summary statistics of the genetic variation observed in the set of genomewide random contigs. All statistics were calculated directly from the joint site frequency spectra (sites that did not pass quality control were masked out)

		Aspidoscelis inornata	*Sceloporus cowlesi*
	Length (bp)	1 776 757	1 429 855
WS	n	9	9
	S	9983	12 308
	π	0.0018	0.0025
	D	0.31	−0.01
DS1	n	9	9
	S	7750	11 693
	π	0.0015	0.0025
	D	0.80	0.25
DS2	n	6	6
	S	9497	11 946
	π	0.0018	0.0027
	D	0.11	−0.17
F_{ST}	WS-DS1	0.13	0.15
	WS-DS2	0.11	0.10
	DS1-DS2	0.15	0.13

Demographic analysis of the Sceloporus cowlesi Populations

All three *S. cowlesi* populations exhibited similar levels of nucleotide diversity (0.25–0.27%, Table 1), with roughly 1.5-fold higher genetic variation than observed in *A. inornata*. Tajima's *D* values ranged from −0.17 to 0.25. The range of pairwise weighted F_{st} values was similar to that found in *A. inornata* (from 0.10 in WS-DS2 to 0.15 in WS-DS1). The *structure* results reported two or three clusters depending on which criterion was used to identify the best value of *K* (Figs 2 and S1B, Supporting information, respectively), highlighting the lower level of differentiation between WS and DS2. However, the three-cluster grouping correctly assigned all individuals to their respective sampling localities. The same pattern of differentiation was observed in the PCA (Fig. 3) where WS and DS2 could only be differentiated on the second principal component. As in *A. inornata*, weighted F_{st} was notably higher within the *Mc1r* region relative to the genomic background in comparisons between White Sands and dark soil populations [0.31 (WS-DS1), 0.20 (WS-DS2)], but not between the two dark soil populations [0.16 (DS1-DS2)].

Both fastsimcoal2 and δaδi analyses predicted the same general demographic model as best fitting the data (Fig. 4), a model with a closer relationship between WS and DS2 and presence of gene flow between the three populations. Although both methods agreed on the tree topology and on the presence of gene flow, there are, unlike in the case of *A. inornata*, notable differences between the parameters estimated by the two methods (Table 2). To test whether these different parameter estimates affected the predictive power of the model, we conducted predictive simulations using both the fastsimcoal2 and *δaδi* estimates and compared their ability to predict the observed data (Figs S4 and S5, Supporting information). The results demonstrated that both methods were indeed equally well calibrated as they correctly predicted the distribution of π, Tajima's *D* and F_{st} in all three populations (Fig. S4, Supporting information).

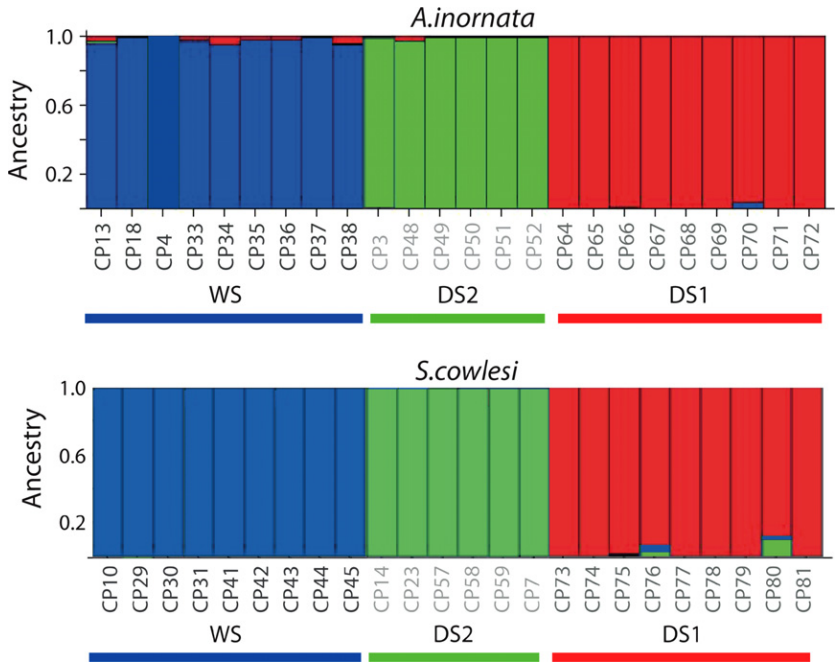

Fig. 2 Estimated population structure as inferred by *structure* for *Aspidoscelis inornata* and *Sceloporus cowlesi*. Each individual is represented by a bar partitioned into *K* coloured segments; the colour of each bar's label indicates the source population, corresponding to Fig. 1: WS (blue), DS1 (red) and DS2 (green). These segments represent the estimated membership fractions of the individual in *K* clusters. At each *K*, ten *structure* runs were performed which generated nearly identical individual membership coefficients. Figures shown for a given *K* are based on the highest probability run.

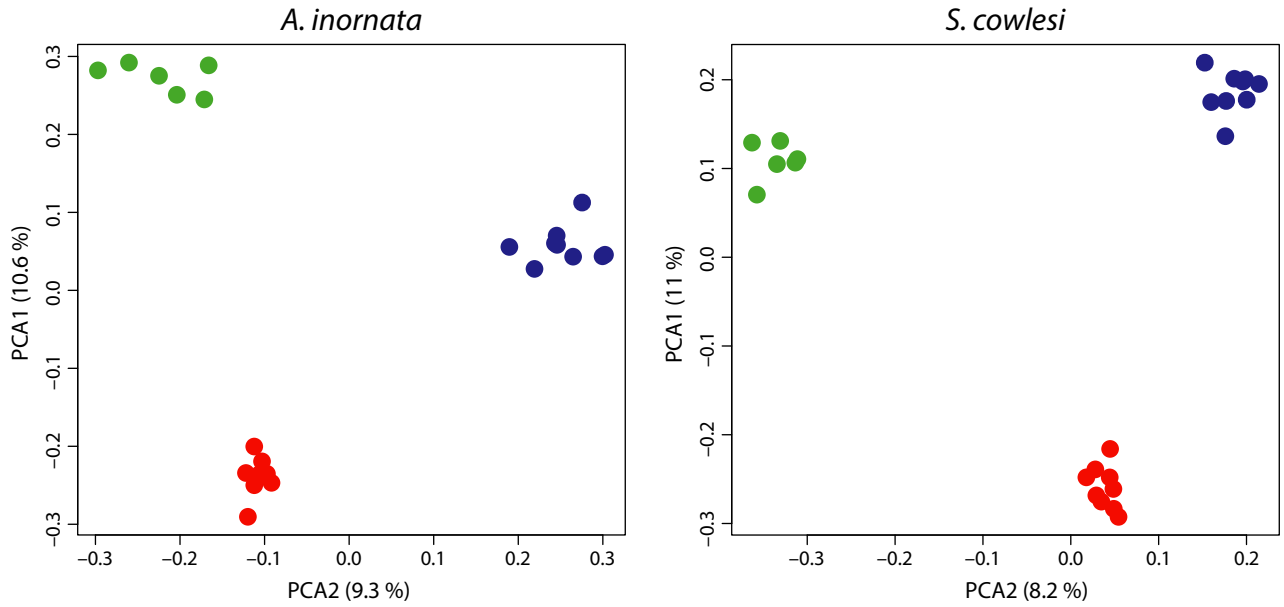

Fig. 3 PCA of sampled populations in *Aspidoscelis inornata* and *Sceloporus cowlesi*; Colours correspond to Fig. 1; WS (blue), DS1 (red) and DS2 (green). Data were thinned to exclude SNPs with an $r^2 > 0.2$ to avoid a strong influence of SNP clusters in the PCA. Percentages indicate the percentage of variance explain by each principal component.

Additionally, both approaches predicted similar single population SFS that matched the observed data well (Fig. S5, Supporting information). It is also necessary to note that when scaling to calendar years, the uncertainty in mutation rate, recombination rate and generation time in these nonmodel organisms has important implications (see Table S2, Supporting information for an example considering the effect of two possible mutation rates and three possible generation times on demographic parameters for each species).

Selection analysis at the Mc1r Locus in Aspidoscelis inornata

Several aspects of the genetic variation observed at the *Mc1r* locus in *A. inornata* stand in sharp contrast with

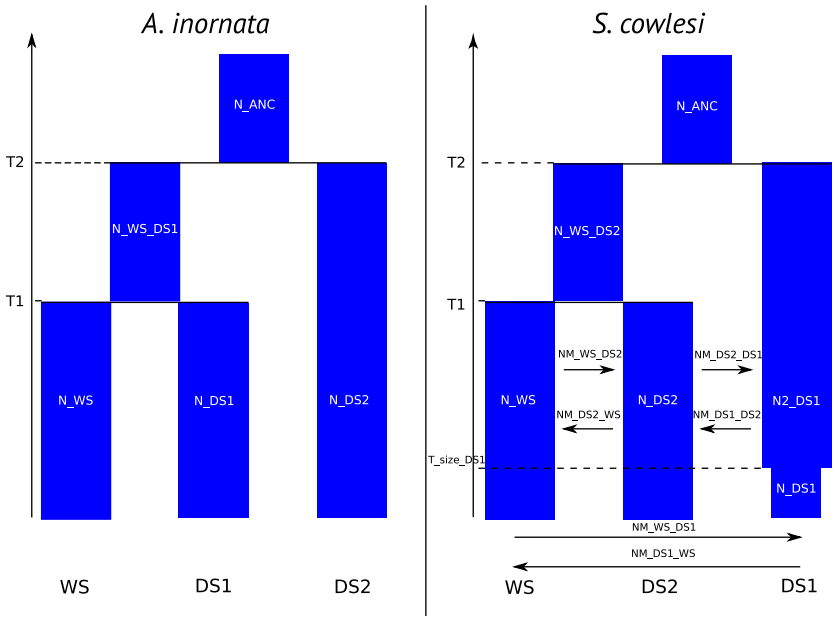

Fig. 4 Best demographic model for *Aspidoscelis inornata* and *Sceloporus cowlesi* as inferred by both δaδi and fastsimcoal2, with parameters defined.

Table 2 Parameter estimates inferred by fastsimcoal2 and δaδi under the best demographic models for *Aspidoscelis inornata* and *Sceloporus cowlesi*. Times are given in years and sizes in number of individuals. A graphical representation of these two demographic models (and parameter definitions) can be found in Fig. 4

	A. inornata		*S. cowlesi*	
	fsc2	δaδi	fsc2	δaδi
N_ANC	327 022	324 114	394 383	420 678
N_WS_DS1	46 478	123 264	–	–
N_WS	49 586	23 392	173 803	20 237
N_DS1	16 104	7443	58 323	15 232
N_DS2	83 463	87 418	256 011	32 068
T1	9627	4538	435 660	7401
T2	15 462	18 168	453 086	254 652
T_SIZE_DS1	–	–	10 656	7401
N2_DS1	–	–	308 492	1 076 768
NE_WS_DS2	–	–	66 690	1 515 572
M_WS_DS1	–		4.01E-06	2.95E-05
M_WS_DS2	–	–	2.73E-06	3.02E-06
M_DS1_WS	–	–	9.30E-07	1.75E-05
M_DS1_DS2	–	–	2.59E-06	2.75E-05
M_DS2_WS	–	–	5.74E-06	3.09E-06
M_DS2_DS1	–	–	2.99E-06	2.75E-05

the diversity observed in the species' genomic background and are consistent with recent and strong positive selection. First, as noted above, the level of genetic differentiation among populations at *Mc1r* was very high compared with the differentiation observed at neutral fragments (Fig. 5). Second, the nucleotide diversity at the *Mc1r* locus in the WS population was below the genomewide average over a region of about 50 kb encompassing the *Mc1r* gene (Fig. 6). Furthermore, only two of nine individuals contributed to most of the variation in this region (CP4 and CP34). If these two individuals are discarded, the seven remaining individuals are almost entirely monomorphic over ~35 kb region (Fig. S6, Supporting information). This reduction in diversity at *Mc1r* is not observed in the dark soil populations (Fig. 6) and is consistent with the expected local reduction in neutral diversity predicted by the selective sweep model (Maynard Smith and Haig 1974). Note that the estimated and observed neutral diversity indices are very similar between all three populations (Table 1), so we do not expect higher levels of genetic drift in WS to be responsible for the lower variation at *Mc1r*. Third, as expected in a region that experienced recent strong positive selection, Tajima's *D* values in the WS population were negative and below the genomic background average. This was not observed in the dark soil populations where *D* profiles were above average (DS1) or in-line (DS2) with their respective background distributions (Fig. 6). To test whether patterns of variation were consistent with a recent event of strong positive selection, we applied the CLR test (Kim & Stephan 2002; Nielsen *et al.* 2005) (Fig. 7). The test was only significant for the WS population and yielded an estimated selection coefficient for the advantageous allele of 9×10^{-4}. This estimation was obtained assuming a recombination rate of 1.5×10^{-9} and an effective population size for WS of 23 392 individuals (Table 2).

This newly identified selective sweep in *A. inornata* colocalized with a nonsynonymous mutation in *Mc1r*

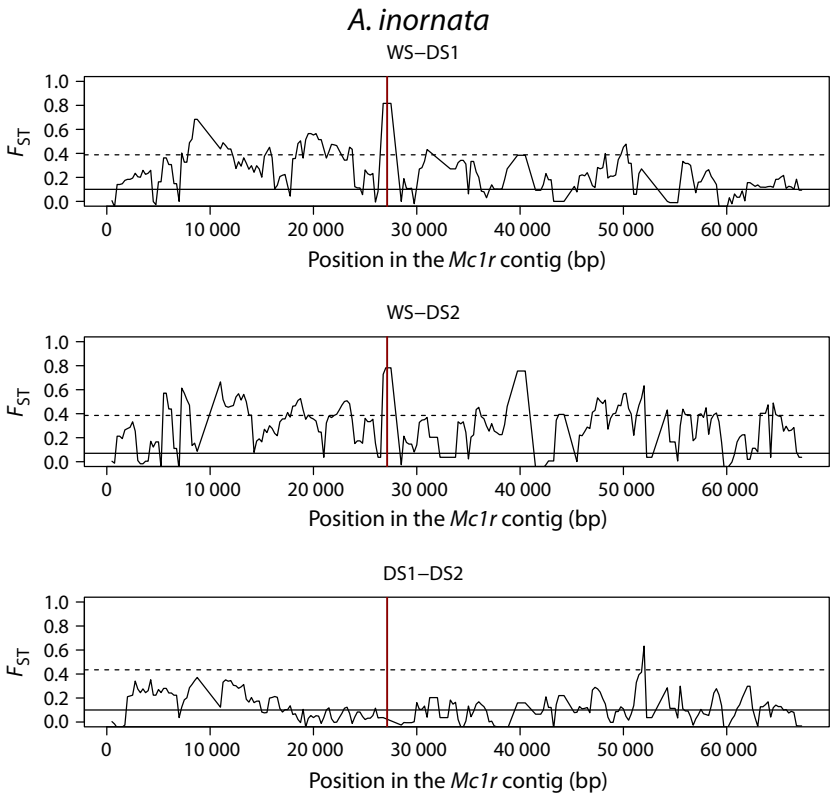

Fig. 5 Genetic differentiation at the *Mc1r* locus in *Aspidoscelis inornata*. Sliding window profile of Weir & Cockerham's (1984) estimator of F_{st} for all pairs of populations as calculated by VCFtools. Window size was 1000 bp and step size 250 bp. Sites that did not pass quality control were masked (using the '–mask' option). The solid horizontal lines represent the average weighted F_{st} across all windows in the genomic background. The dashed horizontal line represents the .975th quantile of the same distribution. The red vertical solid line indicates the position of the nonsynonymous *Mc1r* mutation reported by Rosenblum *et al.* (2010).

responsible for a polarity-changing replacement ($THR^{170}ILE$) that has been previously associated with blanched coloration in *A. inornata* (Rosenblum *et al.* 2010). Consistent with the hypothesis that this mutation plays a major role in the local adaptation of the WS population, we found the frequency of the white allele (T) to be 0.83 (i.e. 15 of 18 gene copies) in our WS sample and absent in DS1 and DS2. This represented the largest difference in allele frequencies between populations in the *Mc1r* region for the WS-DS1 comparison ($F_{st} = 0.82$) and the second largest for WS-DS2 ($F_{st} = 0.78$) (Fig. S7, Supporting information). The three copies of the dark allele (C) were found in CP34 (homozygote) and CP4 (heterozygote), the two individuals contributing to most of the residual variation in the sweep region. Interestingly, these two individuals appear to share the same blanched phenotype as the other samples from the WS population, suggesting the existence of additional loci contributing to the genetic basis of this adaptive trait.

Selection analysis at the Mc1r Locus in Sceloporus cowlesi

In *S. cowlesi*, the *Mc1r* region does not contain a signal for selection as strong as that in *A. inornata*, but several aspects of diversity still suggest a strong selective sweep of the mutation identified by Rosenblum *et al.* (2010). Inspection of polymorphism patterns revealed the presence of strong haplotypic structure in the *Mc1r* alignment (Fig. S7, Supporting information). The four WS individuals that were homozygous for the white allele exhibited dramatically reduced genetic variation across the entire contig (55 kb) compared with individuals homozygous for the dark allele. Heterozygotes were found in WS only, which stands in agreement with the expected dominance of the white allele. F_{st} values only marginally reflected this strong haplotypic differentiation as the white haplotype was not fixed in WS (Fig. S7, Supporting information). The results of the CLR test on this white haplotype subset of WS yielded significant values over the whole sequenced region (Fig. 7). The selection coefficient estimated by the CLR method was 1.1×10^{-3}, assuming a recombination rate of 1.5×10^{-9} and an effective population size of 20 237 (Table 2).

The selective sweep in *S. cowlesi* is in the region of the mutation in *Mc1r* that leads to an amino acid replacement ($HIS^{208}TYR$) and is associated with the blanched phenotype in individuals that are homozygotes or heterozygotes for the white allele (Rosenblum *et al.* 2010). Consistent with the study of Rosenblum *et al.* (2010), this mutation occurred with a frequency of 0.61 in our WS sample (four individuals were

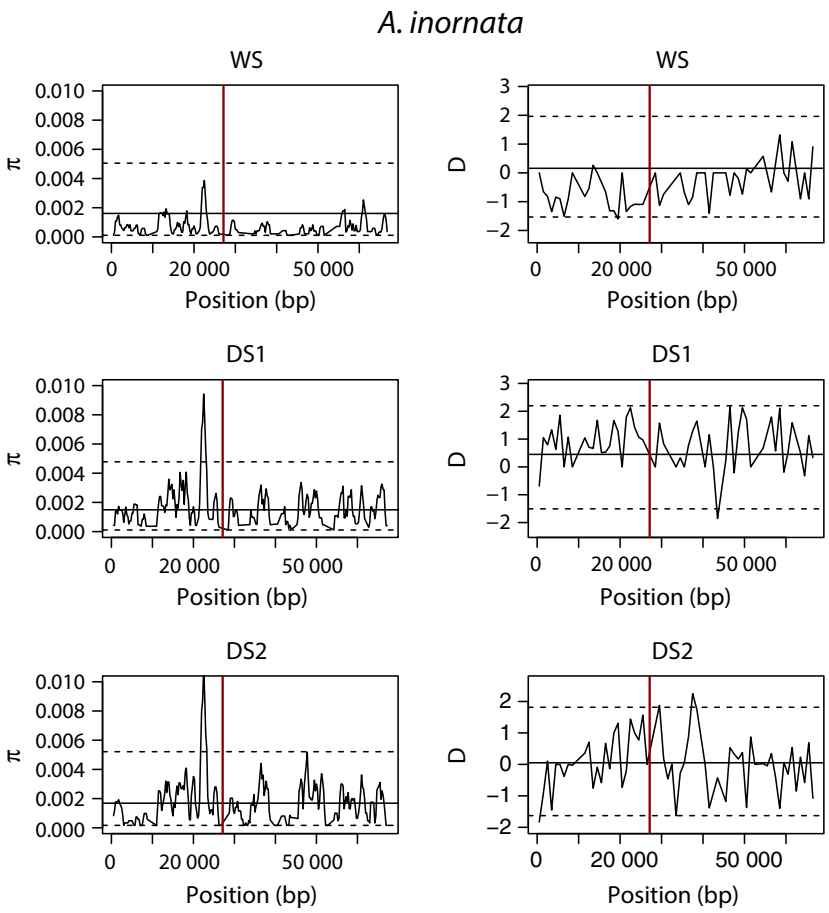

Fig. 6 Nucleotide diversity (π) and Tajima's *D* at the *Mc1r* locus in *Aspidoscelis inornata*. Sliding window profile of nucleotide diversity (π) and Tajima's *D* in the *Mc1r* region as calculated by VCFtools (window size 1000 bp and step size 250 bp). Sites that did not pass quality control were masked (using the '–mask' option). The solid horizontal lines represent the average values of these statistic calculated across all windows in the genomic background. The dashed horizontal lines represent the 0.025th and 0.975th quantiles of the same distribution. The red vertical solid line indicates the position of the nonsynonymous *Mc1r* mutation reported by Rosenblum *et al.* (2010).

homozygotes and three heterozygous) but was absent from both DS1 and DS2. Interestingly, two WS individuals who were homozygous for the dark allele had a light phenotype, suggesting other loci besides *Mc1r* contribute to the blanched phenotype in *S. cowlesi* as well.

ABC estimation of selection coefficients and allele ages

Using an ABC-based approach, we estimated selection coefficients for the putative target of 0.19 based on the inferred fastsimcoal2 model and 0.15 based on the inferred δaδi model in *A. inornata*. In *S. cowlesi*, we estimated selection coefficients for the putative target of 0.12 based on the fastsimcoal2 model and 0.05 based on the δaδi model (Fig. 8). Interestingly, the age of the beneficial mutation was inferred to be young in both species, with estimates ranging from 0.0002 to 0.003 $4N$ generations in *A. inornata* (mean estimate of 900 years), and from 0.01 to 0.001 $4N$ generations in *S. cowlesi* (mean estimate of 1200 years). The posteriors suggest that it may be difficult to distinguish between the ages of these two relatively young sweeps, but we can conclude that the sweeps are young in both species. In fact, given the estimates of effective population sizes, both sweep patterns appear to be significantly younger than the geological age of the White Sands.

Discussion

The White Sands lizards of southern New Mexico offer an outstanding system to understand the demographic and adaptive history associated with colonization of young and novel habitats. Given that multiple species have independently and convergently adapted to the light coloured sand and that the genetic basis of adaptation is known in some species, this system offers insight into the topology of the adaptive landscape and the interplay between selection and demography during colonization. Our sequence capture approach gave us large contigs surrounding the *Mc1r* gene (68 kb long for *Aspidoscelis inornata* and 54 kb long for *S. undulatus*) and large contigs for hundreds of other genomic regions (a total of 13 553 SNPs for *A. inornata* and 20 091 SNPs for *Sceloporus cowlesi*), allowing us to make robust inferences about demography and selection in this system.

Demography. Our findings using hundreds of anonymous loci to estimate the neutral demographic history

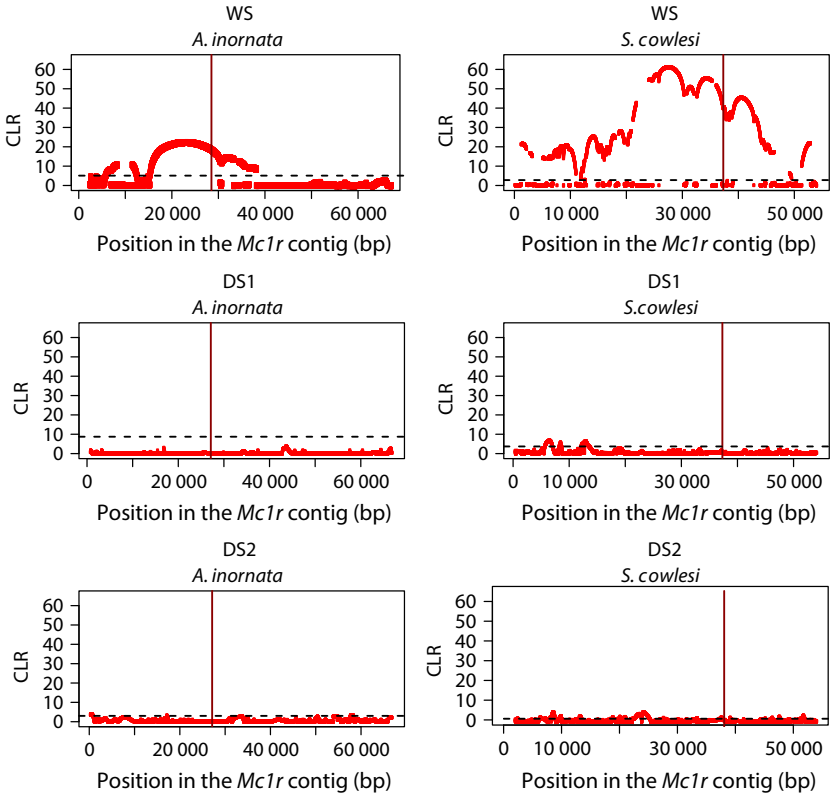

Fig. 7 Likelihood surfaces of the CLR test calculated by *SweeD* for *Aspidoscelis inornata* and *Sceloporus cowlesi*. The dashed horizontal line is the significance threshold of the test for WS (see Methods). The red vertical solid line indicates the position of the nonsynonymous *Mc1r* mutations reported by Rosenblum *et al.* (2010). Individuals that were homozygous for the dark allele of this mutation were excluded from the analysis (see Methods).

of the two species pairs investigated here provide insight into both shared and unique aspects of colonization of a novel habitat. In both *A. inornata* and *S. cowlesi*, all populations sampled were distinguishable from each other, indicating that there is genetic structure over this habitat gradient at a fine spatial scale (Figs 2 and 3). In both species, the White Sands populations also showed a comparable amount of genetic diversity as dark soil populations (Table 1). There is evidence in both species for population size reductions relative to the ancestral population, but this effect was no stronger in White Sands populations than in dark soil populations. Thus, we did not find evidence for dramatic genetic bottlenecks at White Sands, consistent with earlier work in this system that drew from more limited genetic data (Rosenblum *et al.* 2007).

We inferred recent divergence times between White Sands and dark soil populations in both species (Fig. 4, Table 2), consistent with the known geological history of the formation. However, the inferred split time of light and dark populations of *A. inornata* (in which the most recent split was between WS and DS1 ~4500 years ago) was considerably younger than in *S. cowlesi* (in which the most recent split was between WS and DS2 ~7400 years ago). The difference in divergence time estimates between the two species might reflect a more recent colonization of the dunes by *A. inornata* or a limited sampling of dark soil populations for this study. Finally, patterns of gene flow differed between the two focal species. In the species with the more recent split, *A. inornata*, no migration was detected, while in *S. cowlesi* there was strong evidence for ongoing migration (Fig. 4, Table 2).

It is additionally of note that while the two commonly used demographic estimators utilized here agree on important features of tree topology and the presence/absence of migration, there are notable differences particularly in *S. cowlesi* with regard to specific parameter estimates. Perhaps the most important of which is the age of the WS population divergence, with δaδi inferring a more recent split (postdune formation) from DS2, and fastsimcoal2 inferring a more ancient split (prior to dune formation). By conducting simulations of the best estimated models of the two approaches, we have demonstrated that both well explain the observed data – highlighting the fact that there are areas of the demographic parameter space that are equally able to predict our observations. Future work will focus on a more comprehensive sampling of dark soil populations to better understand the ancestry of White Sands populations and refine divergence time estimates.

Selection. Apart from the inherent interest in characterizing the demographic history of colonization in the White Sands lizards, our demographic estimates also provide an important null model for tests of positive selection. We evaluated patterns of molecular evolution around the

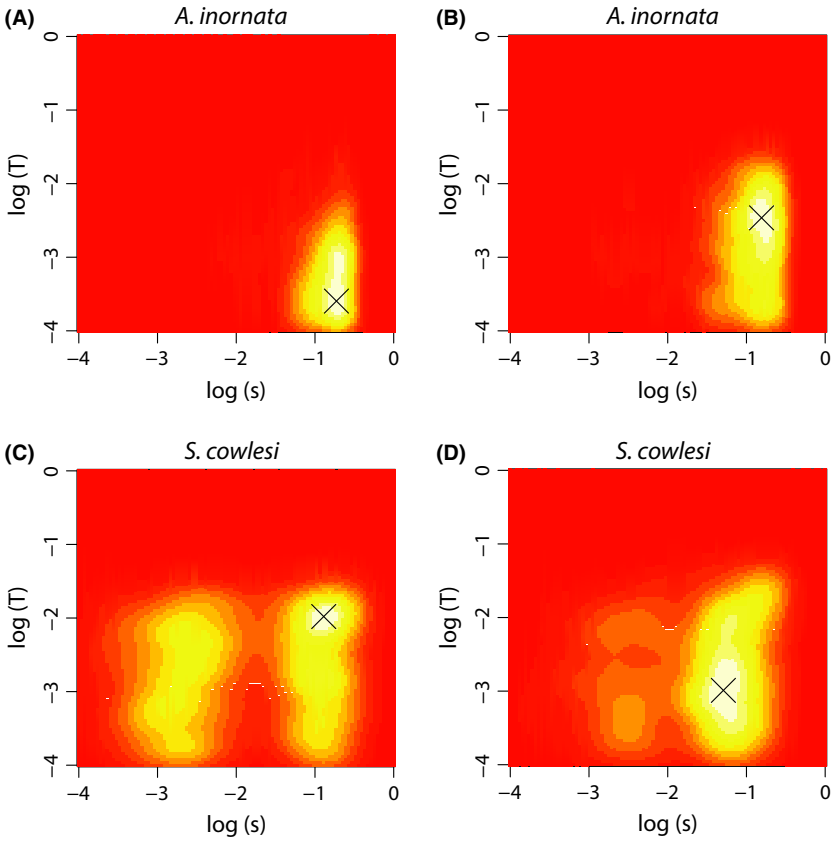

Fig. 8 Estimation of selection coefficient s and allele ages T. Figures show the joint posterior density plots for s and T. Given somewhat different demographic histories estimated between the fastsimcoal2 (Panel A & C) and $\delta a \delta i$ (panel B & D) software, both results are shown for each species. The white, yellow and red colours indicate areas of high, moderate and low joint density, respectively. s and T are drawn from log uniform priors: $log_{10}(s) \sim U(-4, -0.5)$ and $log_{10}(T) \sim U(-4, -0.5)$. Black crosses indicate the modes of the joint posterior distributions, which are at $s = 0.19$ (CI: 0.006–0.3), $T = 0.00025 \times 4N_e$ generations (CI: 0.0001–0.002) based on fastsimcoal2 estimates and $s = 0.16$ (CI: 0.0009–0.3), $T = 0.0034 \times 4N_e$ generations (CI: 0.0001–0.002) based on $\delta a \delta i$ estimates for *Aspidoscelis inornata;* and $s = 0.13$ (CI: 0.0002–0.2), $T = 0.014 \times 4N_e$ generations (CI: 0.0001–0.003) based on fastsimcoal2 estimates and $s = 0.05$ (CI: 0.0003–0.2), $T = 0.001 \times 4N_e$ generations (CI: 0.0001–0.004) based on $\delta a \delta i$ estimates for *Sceloporus cowlesi.*

Mc1r gene, a region hypothesized to be under selection, relative to the genomic background. Based on F_{st} analyses, it was clear that *Mc1r* is much more strongly differentiated between light and dark individuals than was expected based on differentiation across the rest of the genome for both species. Evidence for selection based on patterns of F_{st}, nucleotide diversity and Tajima's D was particularly strong for *A. inornata* (Figs 5 and 6). In addition to F_{st} analyses, we also took a CLR approach to evaluate the likelihood of selection across the *Mc1r* region. In the two dark soil populations sampled for each species, no significant test value was found. However, in light populations of both *A. inornata* and *S. cowlesi*, strongly significant rejections of neutrality were identified (Fig. 7). Interestingly, in both cases, the likelihood surface peaks were centred around two previously described functional variants proposed to play a role in the light phenotype (Rosenblum *et al.* 2010): a polarity-changing replacement in *A. inornata* (THR^{170}ILE) and a replacement in *S. undulatus* (HIS^{208}TYR). Thus, we have now identified specific functional variants associated with colour variation and described signatures of selection in an entire genomic region.

Given the differing colonization histories of these species, it was next of interest to infer the age of the putatively beneficial mutations highlighted by the CLR approach. Taking a newly proposed approximate Bayesian methodology (Ormond *et al.* 2015), we inferred the strength of selection and the age of the light alleles in both species taking into account both the inferred effective population size and the dominance of the underlying mutations (Fig. 8). The strength of selection was estimated to be roughly equally strong in both species, and the ages of both beneficial mutations were estimated to be considerably younger than the age of the White Sands formation itself. This result is highly consistent with the demographic results in *A. inornata*, in which the WS has a recent population split time, consistent with the beneficial allele age. While there is a discrepancy in estimated population split time in *S. cowlesi* between our two inference methods as discussed above, the estimated age of the beneficial allele is indeed young – suggesting that the adaptive event in both species occurred considerably after the formation of the dunes.

Establishing the frequency with which selection acts on rare vs. common variants has become an important focal point in evolutionary genetics. Our results suggest adaptation on *de novo* or rare mutations in both White Sands species. This result is of particular interest given prior theoretical work suggesting that adaptation from standing genetic variation is more likely at White Sands, particularly

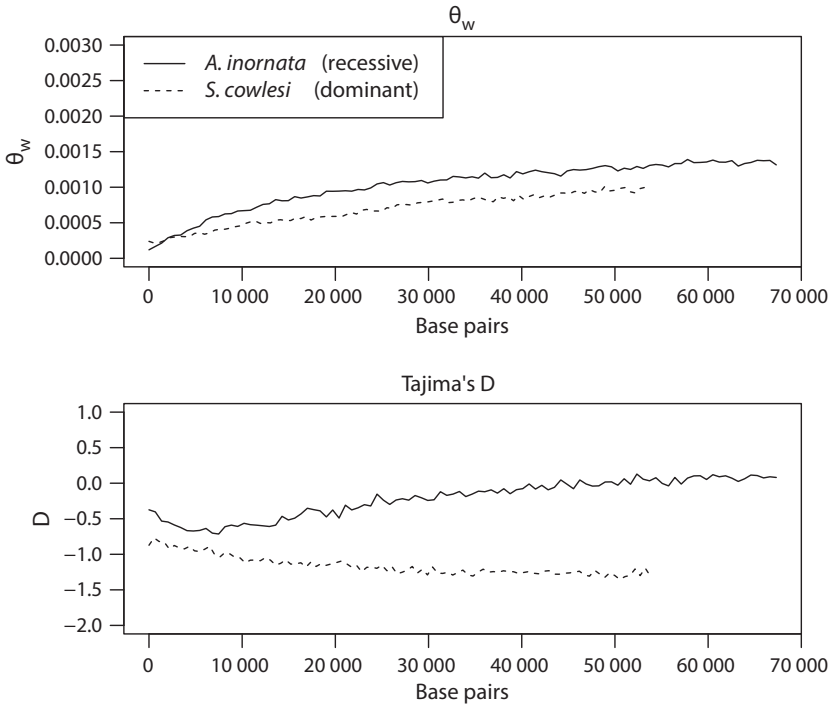

Fig. 9 Predictive simulations under the sweep models inferred in this study for *Aspidoscelis inornata* and *Sceloporus cowlesi* by the ABC method of Ormond *et al*. (2015). The missing values for *S. cowlesi* in the right part of the graph are due to different contig lengths for the *Mc1r* region between the two species. Simulations were performed using the msms program (Ewing & Hermisson 2010).

for the recessive case (Nuismer *et al*. 2012). However, our approach, which leveraged hundreds of SNPs over more than 50 kb in the *Mc1r* gene region, provides a more robust analysis of strength of selection and allele age than has been previously possible. Our inference of selection on rare mutations is based on: (i) the strong CLR signal in both light populations, a test which only has power to detect hard selective sweeps, (ii) the inferred allele ages being considerably younger than the age of the White Sand formation (i.e. the timing of the shift in selection pressure) and (iii) the light allele not being observed as segregating in the dark populations. As it is expected that the light phenotype would be deleterious on the dark soil, it is likely segregating at mutation–selection balance in the dark populations. Given the necessary frequency at which selection on a standing variant results in a soft sweep (i.e. a multiple haplotype fixation) vs. a hard sweep (i.e. a single haplotype fixation) as described by Orr & Betancourt (2001) and Jensen (2014), a soft sweep model is thus unlikely in these populations. However, we have reason to believe that there are as-of-yet unknown variants contributing to the phenotype; therefore, a model of polygenic adaptation cannot be ruled out.

Given the inference of selection around previously identified and functionally validated variants, along with the in-depth demographic estimates, this system provides another unique perspective – namely, the role of dominance. The beneficial light allele appears to be dominant in *S. cowlesi* but recessive in *A. inornata*. Although the mean fixation time of both a recessive and dominant favoured allele is similar for large N and Ns (Van Herwaarden & van der Wal 2002), the impact of a selective sweep in both cases is expected to differ. When selection acts on a recessive beneficial mutation, genetic drift dominates the early phase of the allele trajectory, as the mutation remains invisible to selection until it reaches a frequency at which it may appear in a homozygous recessive state. However, once achieving that frequency, a deterministic trajectory may be entered bringing the allele to fixation. Conversely, for selection acting on a dominant beneficial mutation, the variant may be visible to selection immediately and begin sweeping; however, genetic drift will dominate the later phases of the trajectory as the wild type recessive allele will be invisible to selection when in the heterozygous state. As described by Teshima & Przeworski (2006), these dynamics result in a stronger reduction in diversity near the selected site for recessive mutations, but a wider reduction for dominant mutations. Figure 9 presents simulation results for these two models, for the species-specific parameters estimated here. Although this analysis only represents a single example, our results are indeed qualitatively consistent with theoretical predictions – particularly when considering the width of the significant likelihood surface.

Conclusion

Our study provides a number of important insights into the process of parallel ecological adaptation in a novel

and geologically young environment. While the times of colonization may differ between the focal species, both appear to have colonized the White Sands area after their geological formation, utilizing different genetic mechanisms within *Mc1r*. Both functional and population genetic evidence now strongly support the role of these two identified *Mc1r* variants in shaping the light phenotype. Our results also suggest that other as-of-yet unknown mutations likely play a role in the light adaptation. Thus, future research will seek to identify these additional mutational targets and will expand to other light/dark species pairs across this ecotone to more fully characterize the generality of these conclusions.

Acknowledgements

We thank White Sands National Monument, White Sands Missile Range, Jornada Long-term Ecological Research Station and New Mexico Department of Game and Fish for providing permits and access to field sites. We thank Hopi Hoekstra for input on project planning, Karina Klonoski and Doug Burkett for contributions to field work, Christine Parent, Eveline Diepeveen and Tyler Hether for contributions to laboratory work, Laurent Excoffier for input on the demographic analyses and Kristen Irwin for feedback on the manuscript. Computations were performed at the Vital-IT (http://www.vital-it.ch) Center for high-performance computing of the The Swiss Institute of Bioinformatics (SIB). Funding was provided by a National Science Foundation CAREER grant to EBR (DEB-1054062), and a Swiss National Science Foundation grant and a European Research Council (ERC) Starting Grant to JDJ.

References

Akaike H (1974) A new look at the statistical model identification. *Automatic Control, IEEE Transactions on*, **19**, 716–723.

Barsh GS (1996) The genetics of pigmentation: from fancy genes to complex traits. *Trends in Genetics*, **12**, 299–305.

Bittner TD, King RB, Kerfin JM, Gatten RE (2002) Effects of body size and melanism on the thermal biology of garter snakes. *Copeia*, **2002**, 477–482.

Browning SR, Browning BL (2007) Rapid and accurate haplotype phasing and missing-data inference for whole-genome association studies by use of localized haplotype clustering. *The American Journal of Human Genetics*, **81**, 1084–1097.

Caro TIM (2005) The adaptive significance of coloration in mammals. *BioScience*, **55**, 125–136.

Chan YF, Marks ME, Jones FC *et al.* (2010) Adaptive evolution of pelvic reduction in sticklebacks by recurrent deletion of a *Pitx1* enhancer. *Science*, **327**, 302–305.

Cott HB (1940) *Adaptive Coloration in Animals*. Methuen, London.

Crenshaw JW (1955) The life history of the southern spiny lizard, *Sceloporus undulates undulates* Latreille. *The American Midland Naturalist*, **54**, 257–298.

Crisci JL, Poh Y, Mahajan S, Jensen JD (2013) The impact of equilibrium assumptions on tests of selection. *Frontiers in Genetics*, **4**, 235.

Csillery K, Francois O, Blum MGB (2012) abc: an R package for approximate Bayesian computation (ABC). *Methods in Ecology & Evolution*, **3**, 475–479.

Danecek P, Auton A, Abecasis G *et al.* (2011) The variant call format and VCFtools. *Bioinformatics*, **27**, 2156–2158.

Degenhardt WG, Painter CW, Price AH (1996) *Amphibians and Reptiles of New Mexico*. University of New Mexico Press, Albuquerque, New Mexico.

DePristo M, Banks E, Poplin R *et al.* (2011) A framework for variation discovery and genotyping using next-generation DNA sequencing data. *Nature Genetics*, **43**, 491–498.

Dice LR (1947) Effectiveness of selection by owls of deer mice (*Peromyscus maniculatus*) which contrast in color with their background. Contributions from the Laboratory of Vertebrate Biology of the University of Michigan 34:1–20.

Doebley J (2004) The genetics of maize evolution. *Annual Reviews of Genetics*, **38**, 37–59.

Domingues VS, Poh Y-P, Peterson BK, Pennings PS, Jensen JD, Hoekstra HE (2012) Evidence of adaptation from ancestral variation in young populations of beach mice. *Evolution*, **66**, 3209–3223.

Eizirik E, Yuhki N, Johnson WE, Menotti-Raymond M, Hannah SS, O'Brien SJ (2003) Molecular genetics and evolution of melanism in the cat family. *Current Biology*, **13**, 448–453.

Ellegren H, Sheldon BC (2008) Genetic basis of fitness differences in natural populations. *Nature*, **452**, 169–175.

Evanno G, Regnaut S, Goudet J (2005) Detecting the number of clusters of individuals using the software STRUCTURE: a simulation study. *Molecular Ecology*, **14**, 261126–20.

Ewing G, Hermisson J (2010) MSMS: a coalescent simulation program including recombination, demographic structure and selection at a single locus. *Bioinformatics*, **26**, 2064–2065.

Excoffier L, Foll M (2011) fastsimcoal: a continuous-time coalescent simulator of genomic diversity under arbitrarily complex evolutionary scenarios. *Bioinformatics*, **27**, 1332–1334.

Excoffier L, Dupanloup I, Huerta-Sánchez E, Sousa VC, Foll M (2013) Robust demographic inference from genomic and SNP data. *PLoS Genetics*, **9**, e1003905.

Falush D, Stephens M, Pritchard JK (2003) Inference of population structure: extensions to linked loci and correlated allele frequencies. *Genetics*, **164**, 1567–1587.

Falush D, Stephens M, Pritchard JK (2007) Inference of population structure using multilocus genotype data: dominant markers and null alleles. *Molecular Ecology Notes*, **7**, 574–578.

Gutenkunst RN, Hernandez RD, Williamson SH, Bustamante CD (2009) Inferring the joint demographic history of multiple populations from multidimensional SNP frequency data. *PLoS Genetics*, **5**, e1000695.

Hoekstra HE, Hirschmann RJ, Bundey RA, Insel PA, Crossland JP (2006) A single amino acid mutation contributes to adaptive beach mouse color pattern. *Science*, **313**, 101–104.

Hubisz MJ, Falush D, Stephens M, Pritchard JK (2009) Inferring weak population structure with the assistance of sample group information. *Molecular Ecology Resources*, **9**, 1322–1332.

Ihle S, Ravaoarimanana I, Thomas M, Tautz D (2006) An analysis of signatures of selective sweeps in natural populations of the house mouse. *Molecular Biology & Evolution*, **23**, 790–797.

Jensen JD (2014) On the unfounded enthusiasm for soft selective sweeps. *Nature Communications*, **5**, 5281.

Jensen JD, Kim Y, DuMont VB, Aquadro CF, Bustamante CD (2005) Distinguishing between selective sweeps and demography using DNA polymorphism data. *Genetics*, **170**, 1401–1410.

Jensen JD, Wong A, Aquadro CF (2007) Approaches for identifying targets of positive selection. *Trends in Genetics*, **23**, 568–577.

Kaufman DW (1974) Adaptive coloration in *Peromyscus polionotus*: Experimental selection by owls. *Journal of Mammalogy*, **55**, 271–283.

Kettlewell B (1973) *The Evolution of Melanism: The Study of a Recurring Necessity; With Special Reference to Industrial Melanism in the Lepidoptera*. Clarendon Press, Oxford.

Kijas JMH, Wales R, Tornsten A, Chardon P, Moller M, Andersson L (1998) Melanocortin receptor 1 (MC1R) mutations and coat color in pigs. *Genetics*, **150**, 1177–1185.

Kim Y, Stephan W (2002) Detecting a local signature of genetic hitchhiking along a recombining chromosome. *Genetics*, **160**, 765–777.

Kocurek G, Carr M, Ewing R, Havholm KG, Nagar YC, Singhvi AK (2007) White Sands Dune Field, New Mexico: age, dune dynamics and recent accumulations. *Sedimentary Geology*, **197**, 313–331.

Langford RP (2003) The Holocene history of the White Sands dune field and influences on eolian deflation and playa lakes. *Quaternary International*, **104**, 31–39.

Li H, Handsaker B, Wysoker A *et al.* (2009) The sequence alignment/map format and SAMtools. *Bioinformatics*, **25**, 2078.

Linnen CR, Poh Y-P, Peterson BK *et al.* (2013) Adaptive evolution of multiple traits through multiple mutations at a single gene. *Science*, **339**, 6125.

Lowe CH, Norris KS (1956) A subspecies of the lizard *Sceloporus undulates* from the White Sands of New Mexico. *Herpetologica*, **12**, 125–127.

Luke CA (1989) Color as a phenotypically plastic character in the side-blotched lizard, *Uta stansburiana*, Ph.D. dissertation. University of California, Berkeley.

Lunter G, Goodson M (2011) Stampy: a statistical algorithm for sensitive and fast mapping of Illumina sequence reads. *Genome Research*, **21**, 936.

Mackay TFC, Stone EA, Aryoles JF (2009) The genetics of quantitative traits: challenges and prospects. *Nature Reviews Genetics*, **10**, 565–577.

Magoc T, Salzberg SL (2011) FLASH: fast length adjustment of short reads to improve genomic assemblies. *Bioinformatics*, **27**, 2957–2963.

Majerus M (1998) *Melanism: Evolution in Action*. Oxford University Press, Oxford.

Marklund L, Moller MJ, Sandberg K, Andersson L (1996) A missense mutation in the gene for melanocyte-stimulating hormone receptor (MCIR) is associated with the chestnut coat color in horses. *Mammalian Genome*, **7**, 895–899.

Mathew LA, Jensen JD (2015) Evaluating the ability of the pairwise joint site frequency spectrum to co-estimate selection and demography. *Frontiers Genetics*, **6**, 268.

Maynard Smith J, Haigh J (1974) The hitch-hiking effect of a favourable gene. *Genetic Research*, **23**, 23–35.

McKenna A, Hanna M, Banks E *et al.* (2010) The genome analysis toolkit: a MapReduce framework for analyzing next-generation DNA sequencing data. *Genome Research*, **20**, 1297.

Meiklejohn CD, Kim Y, Hartl DL, Parsch J (2004) Identification of a locus under complex positive selection in *Drosophila simulans* by haplotype mapping and composite-likelihood estimation. *Genetics*, **168**, 265–279.

Mundy NI, Badcock NS, Hart T, Scribner K, Janssen K, Nadeau NJ (2004) Conserved genetic basis of a quantitative plumage trait involved in mate choice. *Science*, **303**, 1870–1873.

Nachman MW, Hoekstra HE, D'Agostino SL (2003) The genetic basis of adaptive melanism in pocket mice. *Proceedings of the National Academy of Sciences, USA*, **100**, 5268–5273.

Naduvilezhath L, Rose LE, Metzler D (2011) Jaatha: a fast composite-likelihood approach to estimate demographic parameters. *Molecular Ecology*, **20**, 2709–2723.

Newton JM, Wilkie AL, He L *et al.* (2000) Melanocortin 1 receptor variation in the domestic dog. *Mammalian Genome*, **11**, 24–30.

Nielsen R, Williamson S, Kim Y, Hubisz MJ, Clark AG, Bustamante C (2005) Genomic scans for selective sweeps using SNP data. *Genome Research*, **15**, 1566–1575.

Nielsen R, Paul JS, Albrechtsen A, Song YS (2011) Genotype and SNP calling from next-generation sequencing data. *Nature Reviews Genetics*, **12**, 443–451.

Norris KS (1967) Color adaptation in desert reptiles and its thermal relationships. In: *Lizard Ecology: A Symposium* (ed. Milstead WW), pp. 162–229. University of Missouri Press, Columbia, Missouri.

Norris KS, Lowe CH (1964) An analysis of background colormatching in amphibians and reptiles. *Ecology*, **45**, 565–580.

Nuismer SL, MacPherson A, Rosenblum EB (2012) Crossing the threshold: gene flow, dominance, and the critical level of standing genetic variation required for adaptation to novel environments. *Journal of Evolutionary Biology*, **25**, 2665–2671.

Olave M, Avila LJ, Sites JW, Morando M (2015) Model-based approach to test hard polytomies in the *Eulaemus* clade of the most diverse South American lizard genus *Liolaemus* (Liolaemini, Squamata). *Zoological Journal of the Linnean Society*, **174**, 169–184.

Orr HA, Betancourt AJ (2001) Haldane's sieve and adaptation from the standing genetic variation. *Genetics*, **157**, 875–884.

Pavlidis P, Jensen JD, Stephan W, Stamatakis A (2012) A critical assessment of storytelling: gene ontology categories and the importance of validating genomic scans. *Molecular Biology & Evolution*, **29**, 3237–3248.

Pavlidis P, Zivkovic D, Stamatakis A, Alachiotis N (2013) SweeD: likelihood-based detection of selective sweeps in thousands of genomes. *Molecular Biology & Evolution*, **30**, 2224–2234.

Poh Y-P, Domingues VS, Hoekstra HE, Jensen JD (2014) On the prospect of identifying adaptive loci in recently bottlenecked populations. *PLoS ONE*, **9**, e110579.

Pollinger JP, Bustamante CD, Fledel-Alon A, Schmutz S, Gray MM, Wayne RK (2005) Selective sweep mapping of genes with large phenotypic effects. *Genome Research*, **15**, 1809–1819.

Pritchard JK, Stephens M, Donnelly P (2000) Inference of population structure using multilocus genotype data. *Genetics*, **155**, 945–959.

Przeworski M (2002) The signature of positive selection at randomly chosen loci. *Genetics*, **160**, 1179–1189.

Reusch TBH, Haeberli MA, Aeschlimann PB, Milinski M (2001) Female sticklebacks count alleles in a strategy of sexual

selection explaining MCH polymorphism. *Nature*, **415**, 300–302.
Rosenberg NA, Burke T, Elo K *et al.* (2001) Empirical evaluation of genetic clustering methods using multilocus genotypes from 20 chicken breeds. *Genetics*, **159**, 699–713.
Rosenblum EB (2006) Convergent evolution and divergent selection: lizards at the White Sands ecotone. *The American Naturalist*, **167**, 1–15.
Rosenblum EB, Harmon LJ (2011) "Same same but different": replicated ecological speciation at White Sands. *Evolution*, **65**, 946–960.
Rosenblum EB, Hoekstra HE, Nachman MW (2004) Adaptive reptile color variation and the evolution of the *Mc1r* gene. *Evolution*, **58**, 1794–1808.
Rosenblum EB, Hickerson M, Moritz C (2007) A multilocus perspective on colonization accompanied by selection and gene flow. *Evolution*, **61**, 2971–2985.
Rosenblum EB, Rompler H, Schoneberg T, Hoekstra HE (2010) Molecular and functional basis of phenotypic convergence at white lizards at White Sands. *Proceedings of the National Academy of Sciences, USA*, **107**, 2113–2117.
Smit AFA, Hubley R, Green P (2013–2015) RepeatMasker Open-4.0 Available from: http://www.repeatmasker.org.
Smith HM (1943) *The White Sands Earless Lizard*. Zoological Series of the Field Museum of Natural History, Chicago, Illinois.
Stapley J, Reger J, Feulner PG *et al.* (2010) Adaptation genomics: the next generation. *Trends in Ecology and Evolution*, **25**, 705–712.
Stinchcombe JR, Hoekstra HE (2008) Combining population genomics and quantitative genetics: finding the genes underlying ecologically important traits. *Heredity*, **100**, 158–170.
Tajima F (1989) Statistical method for testing the neutral mutation hypothesis by DNA polymorphism. *Genetics*, **123**, 585–595.
Takeuchi S, Suzuki H, Yabuuchi M, Takahashi S (1996) A possible involvement of melanocortin 1-receptor in regulating feather color pigmentation in the chicken. *Biochimica et Biophysica Acta (BBA)-Gene Structure and Expression*, **1308**, 164–168.
Teshima KM, Przeworski M (2006) Directional positive selection on an allele of arbitrary dominance. *Genetics*, **172**, 713–718.
Thayer GH (1909) *Concealing—Coloration in the Animal Kingdom: An Exposition of the Laws of Disguise Through Color and Pattern*. Macmillan, New York.
The 1000 Genomes Project Consortium (2010) A map of human genome variation from population-scale sequencing. *Nature*, **467**, 1061–1073.
Theron E, Hawkins K, Bermingham E, Ricklefs RE, Mundy NI (2001) The molecular basis of an avian plumage polymorphism in the wild: a melanocortin-1-receptor point mutation is perfectly associated with the melanic plumage morph of the bananaquit, *Coereba flaveola*. *Current Biology*, **11**, 550–557.
Thornton K, Andolfatto P (2006) Approximate Bayesian inference reveals evidence for a recent, severe bottleneck in a Netherlands population of *Drosophila Melanogaster*. *Genetics*, **172**, 1607–1619.
Thornton KR, Jensen JD (2007) Controlling the false-positive rate in multilocus genome scans for selection. *Genetics*, **175**, 737–750.
Van der Auwera GA, Carneiro MO, Hartl C *et al.* (2013) From FastQ data to high-confidence variant calls: the genome analysis toolkit best practices pipeline. *Current Protocols*, **43**, 11.10.1–11.10.33.
Van Herwaarden OA, van der Wal NJ (2002) Extinction time and age of an allele in a large finite population. *Theor Pop Biol*, **61**, 311–318.
Venables WN, Ripley BD (2002) *Modern Applied Statistics With S*. Springer, New York.
Wegmann D, Leuenberger C, Excoffier L (2009) Efficient approximate Bayesian computation coupled with Markov chain Monte Carlo without likelihood. *Genetics*, **182**, 1207–1218.
Weir BS, Cockerham CC (1984) Estimating F-statistics for the analysis of population structure. *Evolution*, **38**, 1358–1370.
Zheng X, Levine D, Shen J, Gogarten SM, Laurie C, Weir BS (2012) A high-performance computing toolset for relatedness and principal component analysis of SNP data. *Bioinformatics*, **28**, 3326–3328.

E.B.R. and J.D.J. designed and oversaw the research; K.M.H. collected data; S.L., S.P.P., M.L.S., S.S.H., L.O. and V.C.S. analyzed data; S.L., S.P.P., L.O., J.D.J. and E.B.R. interpreted the data and wrote the manuscript.

Data accessibility

Molecular data have been accessioned into the NCBI Sequence Read Archive under the BioProject PRJNA291308 (SRP061970), and NimbleGen capture probe sequences have been accessioned to Dryad doi:10.5061/dryad.m0jk7.

Supporting information

Additional supporting information may be found in the online version of this article.

Table S1 (a) *Aspidoscelis inornata* samples and statistics of mapped coverage. (b) *Sceloporus cowlesi* samples and statistics of mapped coverage.

Table S2 An example of the effects of uncertainty in mutation rate (two rates given) and generation time (three times given) on estimated demographic parameters.

Fig. S1 Left: Mean log posterior probability of the data, L(K), in (A) *Aspidoscelis inornata* and (B) *Sceloporus cowlesi*.

Fig. S2 Predictive distributions of 1000 simulated values of π, Tajima's D, and F_{st} under the best demographic model for *Aspidoscelis inornata* as inferred by fastsimcoal2 (solid line) and *δaδi* (dashed line).

Fig. S3 Predictive distributions of 1000 simulated site frequency spectra under the best demographic model for *Aspidoscelis inornata* as inferred by fastsimcoal2 (dark gray) and *δaδi* (light gray).

Fig. S4 Predictive distributions of 1000 simulated values of π, Tajima's D, and F_{st} under the best demographic model for *Sceloporus cowlesi* as inferred by fastsimcoal2 (solid line) and *δaδi* (dashed line).

Fig. S5 Predictive distributions of 1000 simulated site frequency spectra under the best demographic model for *Sceloporus cowlesi* as inferred by fastsimcoal2 (dark gray) and *δaδi* (light gray).

Fig. S6 Graphical representation of the genetic variation in the contig encompassing the *Mc1r* gene in *Aspidoscelis inornata*.

Fig. S7 Per site weighted F_{st} values in the *Mc1r* region in *Aspidoscelis inornata* (Weir and Cockerham's F_{st}).

Fig. S8 Graphical representation of the genetic variation in the contig encompassing the *Mc1r* gene in *Sceloporus cowlesi*.